Microchemical Journal 157 (2020) 104973

Contents lists available at ScienceDirect

Microchemical Journal

journal homepage: www.elsevier.com/locate/microc

Greenly synthesized silver nanoparticles for supercapacitor and electrochemical sensing applications in a 3D printed microfluidic platform

Mary Salve, Aurnab Mandal, Khairunnisa Amreen, Prasant Kumar Pattnaik, Sanket Goel*

MEMS, Microfluidics and Nanoelectronics Laboratory, Department of Electrical and Electronics Engineering, Birla Institute of Technology and Science, Hyderabad 500078, India

ARTICLE INFO

Keywords:
Green synthesis
Silver nanoparticle
3D printed microfluidics platform
Supercapacitor

ABSTRACT

Herein, Silver nanoparticles (AgNPs) decorated pencil graphite electrodes (PGEs), with assimilation of Chitosan (CS), as a versatile electrode material for supercapacitor and electrochemical sensing application have been reported. The AgNPs were prepared by employing a green synthesis method using marigold flower ꞩ extract. Marigold flower contains lutein, which can be used as a reductant. The morphology and crystal structure of the prepared nanomaterial was characterized by Field emission scanning electron microscopy (FESEM), Elemental Dispersive X-Ray Spectroscopy (EDX), Fourier transform infrared spectrometer (FTIR), X-ray diffraction (XRD), UV-VIS Spectrophotometer and X-ray photoelectron spectroscopy (XPS). The prepared hybrid material, PGE/AgNPs/CS was utilized in an electrochemical 3D printed microfluidic device for supercapacitor and electrochemical sensing of H_2O_2. As a supercapacitor, the device provided a remarkable storage capacity of 367.16 mF cm^{-2}at a current density of 1 mA cm^{-2} with high cyclic stability over 1500 charge-discharge cycle. Subsequently, H_2O_2 sensing with the same electrode in a three-electrode microfluidic system gave a LOD of 0.52 μM within a linear range of 1-10 μM. In addition, the effect of common interfering species, including ascorbic acid (AA), uric acid (UA) dopamine (DA) and xanthine (XN) were thoroughly investigated. Thus, the prepared hybrid electrode material showed excellent electrochemical activity for the supercapacitor and electrochemical sensing of H_2O_2, which can be further assessed for other relevant applications.

1. Introduction

Over the past few decades, exploration of novel methods to synthesize metal nanoparticles has attracted an immense attention of researchers because of their unique optical, thermal and electronic properties, and has an extensive application in drug delivery, information storage, magnetic and optoelectronic [1,2].There are various methods for synthesizing metal nanoparticles such as ion sputtering, chemical reduction, sol-gel [3,4]. All these methods are quite expensive and hazardous for the environment. Although nanocrystalline silver particles have great application in the field of antimicrobial, diagnostic, biomolecular detection, therapeutics and micro-electronics [5–7], yet there is a need of the commercially economical, feasible and environment-friendly method of synthesis. With this goal, green synthesis method, harnessing plant extract like roots, leaves, flower or fruit as reductants and stabilizing agents for metal nanoparticle synthesis, has received great response in diverse research fields. The green synthesis method has an advantage over other approaches as it is inexpensive, eco-friendly and reproducible [8,9]. In the present work, marigold flower extract, consisting of lutein as 95% of the component, assists the reduction of Ag^+ ions to give AgNPs [10].

Silver nanoparticles are extensively used in the field of electrochemical energy storage applicationas it gives high chemical stability, high electronic conductivity, surface chemical properties [11,12]. Owing to these properties, AgNPs have the potential to be used as supercapacitors and energy storage devices. Supercapacitors are considered to be one of the newest innovations in the field of electrical energy storage. With characteristics like high power density, fast charge-discharge life, low equivalent series resistance (ESR) and low-cost maintenance, there is an increase in demand of supercapacitors in electric equipment and digital communication [13–15]. Generally, the electrode materials used in supercapacitor are conducting polymer, nanocarbon and transition metal oxide. The fundamental mechanism of energy storage in a supercapacitor is achieved either by electrical double-layer capacitive (EDLC) based on nanocarbon electrode material or by pseudocapacitive based on Faradic material like transition metal oxide or conducting polymer [16–18]. Hybrid material, like carbon, while combining with conducting polymer or metal oxide, gives the

* Corresponding author.
E-mail address: sgoel@hyderabad.bits-pilani.ac.in (S. Goel).

https://doi.org/10.1016/j.microc.2020.104973
Received 9 January 2020; Received in revised form 24 April 2020; Accepted 27 April 2020

advantage of both EDLC and pseudocapacitor [19–21]. However, the disadvantage of a conducting polymer, while preparing material for supercapacitor application, is its poor stability in charge-discharge cycle due to the redox sites. Even though carbon material has low capacitance value, they have a better life cycle in comparison to the conducting polymers [22].

On the other hand, carbon materials, are often embedded with metal or metal oxide as a promising electrode material for supercapacitor applications [23]. Among various carbon materials, pencil graphite electrode (PGE) is attractive with distinctive advantages like cost-effectiveness, easy availability and reasonably good electrical conductivity. PGE surface has a rough structure as it contains a regularly ordered graphitized layer which leads to ease of modification with reproducibility [24].

The electrode material fabricated by combining PGE and AgNPs can boost the performance of the prepared composite electrode electrochemically. Reports are available on AgNPs and carbon material based composite electrode for supercapacitor application. Liu et al. have grown Ag nanoparticle directly on the porous material substrate as a composite electrode for supercapacitor application [25]. The developed electrode provided a specific capacitance of 517.5 F/g and an outstanding cycle stability of 85.6% retention after 3000 cycles. Das et al. synthesized silver polypyrrole / graphene nanocomposite as an electrode material for supercapacitor application. The developed composite gives a high specific capacitance of 472 F/g at a 0.5 A/g current density. Reports are also available on green synthesis technique for the preparation of AgNPs for supercapacitor and electrochemical application [11]. Chen et al. synthesized AgNPs by reduction of silver nitrate with vitamin C as a nature-friendly reducing agent. The synthesized nanoparticle with polyaniline nanofiber as a nano composite gave an excellent capacitive performance with 553 F/g specific capacitance [8].

Therefore, the incorporation of AgNPs processed using green synthesis techniques on PGE has a strong potential to increase the electrical conductivity and electrochemical storage capacity. Many reports indicate that hydrophilicity of an electrode surface enhances the supercapacitive properties of the active material [26]. The electrode having the property of good wettability gives better penetration of electrolyte into the active surface. Sun et al. showed that assimilation of chitosan (CS) to an electrode material led to better hydrophilic properties as it has the ability to form hydrogen bonding with inherent amine and hydroxyl groups [27]. In the present work, the aforementioned unique advantage of CS with PGE/AgNPs have been combined to investigate its supercapacitor properties and electrochemical sensing using 3DP microfluidic device.

In further, the prepared PGE/AgNPs/CS was explored for electrocatalytic detection activity towards hydrogen peroxide (H_2O_2). H_2O_2 detection has become extremely important in the past few years due to its wide application in food industries, cleaning product, cosmetics, clinic, drugs and environmental analysis [28,29]. H_2O_2 and its derivatives are powerful oxidizing agents that can be used for synthesizing organic compounds and treatment of environmental pollutant. Determining H_2O_2 concentration using electrochemistry has proven to be inexpensive and effective way to investigate the reaction of the substances. A number of electrochemical sensors with and without enzyme were developed for H_2O_2 sensing, but they are relatively costly and unstable. To avoid the drawback of enzyme-based sensing, a novel electrode based on nanomaterial gives better enzyme imitative properties.

Microfluidics offers an easy and instant sensing platform to identify particular biomolecules. From the last two decades, several microfluidic platforms has shown a great potential to meet the desire of low sample volume, cost-effective, rapid analysis and enhanced reaction reliability and reproducibility. Earlier microfluidic devices for rapid production were made using poly(dimethylsiloxane) (PDMS), but prototype development and cost were the limiting factors. 3D-printing enables rapid prototyping of single unit devices by avoiding the use of expensive masks that are necessary for the fabrication using lithography and soft-lithography. Herein, a 3D printed microfluidics platform has been developed for effective electrochemical sensing of H_2O_2 and for supercapacitor application; using the fabricated PGE/AgNPs/CS as a working, Ag/AgCl as reference and platinum wire as a counter electrode.

2. Experimental section

2.1. Chemicals, materials and instrumentation

All the chemicals were of analytical reagent grade and were used without any further purification. Hydrochloric acid (HCl) 35%, Potassium chloride (KCl), Acetic acid(CH_3COOH), Chitosan (CS), Hydrogen peroxide (H_2O_2) 30% and Silver nitrate $Ag(NO)_3$ were obtained from Sigma (St.Louis, MO, USA). Absolute ethanol was obtained from S.D Fine Chemical Limited (Mumbai, India). 0.1M KCl-HCl (pH = 2) was used as a supporting electrolyte. Deionized water (DI) collected from milli-Q was used for aqueous solution preparation. The commercially available pencil lead (2mm, 2B) obtained from Camlinwas obtained from local stationery. Electrochemical measurements were carried out with an electrochemical analyser (SP-150, Bio-Logic, electrochemical workstation (France)). The pH meter from Oakton was used for measuring the accurate pH value of the required solution. The ultra-sonication water bath was obtained from life-care. The CIC-15A hot air oven was obtained from Cintex Industrial Corporation (Mumbai, India). Remi R-4C Laboratory Centrifuge was obtained from m-LABS. ApreoLoVac Field emission scanning electron microscope (FE-SEM) was used for microscopic analysis of the developed nanoparticle. Likewise, FTIR-4200 from Jasco, Rigaku Ultima IV X-ray Diffractometer (XRD), UV-VIS Spectrophotometer V-650 JASCO, Thermo scientific K-Alpha X-ray Photoelectron Spectrometer (XPS) were used for FTIR, XRD,UV-Vis, XPS analysis.

2.2. Procedure

2.2.1. Preparation of the flower extract

Tagetes erecta (Marigold) flowers were collected from a local market in Hyderabad, India. The flower petals were washed and then dried in a hot air oven at 60 °C. 5 g of dried petals were refluxed in a 100ml of distilled water with 4–5 drops of 1 M HCl for an hour with continuous magnetic stirring at 80 °C temperature. The extract was cooled to room temperature and filtered out, giving a dark red filtrate solution (**Scheme 1.**).

2.2.2. One pot synthesis of silver nanoparticles

0.5 mM solution of $Ag(NO)_3$ was prepared in 50 mL DI water. The obtained solution $Ag(NO)_3$ was mixed in 1:1 ratio with the flower extract. The resulting solution was stored overnight in a dark chamber at a room temperature [5]. The Ag^+ ions were reduced to Ag nanoparticles which were observed by the change in color from dark red to orange. Following this, the solution was centrifuged (10000 RPM for 30 min), thereby the particles got settled down at the bottom, whereas the supernatant was discarded. The filtered nanoparticles were washed using 90% ethanol and deionized water for several times and then dispersed in 1ml of ethanol solution using an ultrasonicator for an hour.

2.2.3. Design and fabrication of 3D printed microfluidics platform

3D printing gives a fast and simple way to fabricate microfluidic devices directly from the computer-aided software. A commercial 3D-printer based on fused deposition modelling (Flashforge) was used to print the microfluidic-based platform with ABS filament of 1.75 mm. Using 123D design software, the computer-aided design was created, and the file was exported in .stl format, compatible with the 3D printer software. The design was printed with an optimized extruder temperature of 240 °C, bed temperature as 120°C, infill 100% and a layer

height of 100mm. Here, two 3D printed devices were fabricated that can be used for electrochemical sensing and supercapacitor applications. The fluidic device of total size 40 mm × 18 mm × 5 mm with microchannel of a rectangular reservoir of size 30mm × 4mm × 2mm with inlet holes for the electrode was realized (PGE, Pt and AgCl electrode). The channel was bonded with the glass slide to get a transparent window using a double sided tape.

2.2.4. Preparation of electrode and electrochemical measurement

The supercapacitor PGE was wrapped with non-conductive parafilm (Tarson) by leaving the disc portion (i.e. bottom part) for the electrochemical studies. The exposed surface was equalized by polishing it on Silicon Carbide Waterproof Abrasive Sandpaper Sheet 1500 Cw. On the exposed surface of PGE (2mm), AgNPs solution (3 μL) was drop-casted twice followed by a single layer of CS (2 μL). After each layer of drop-casting, it was allowed to dry at ambient temperature for 2 h.

The developed 3D printed microfluidics platform for two, and three-electrode setup was used for supercapacitor and electrochemical sensing application using 500 μL of working solution (**Scheme 2.**). The electrochemical storage properties of the prepared material were characterized using cyclic voltammetry (CV), electrochemical impedance spectroscopy (EIS), galvano static charge-discharge (GCD), capacitive retention in 1M HCl-KCl (pH = 2) aqueous solution. EIS measurements were carried out in the range of $0.01 \sim 10^5$ Hz with an amplitude of 10mV. The three-electrode system consisted of a modified PGE/AgNPs/CS, Pt and Ag/AgCl (1M HCl-KCl) as the working, counter and reference electrodes. In a three-electrode configuration the areal capacitance values were calculated from the GCD curves using equations:

$$C = I\,\Delta t / S\,\Delta V \quad (1)$$

Where I is discharging current in mA-cm^{-2}, Δt is the discharging time in seconds, ΔV is the potential window and S is the active area of the working electrode in cm^2.

3. Result and discussion

3.1. Characterization of the silver nanoparticles

In order to study the topographical morphology of the synthesized AgNPs, a field emission scanning electron microscope (FE-SEM) was used.The FE-SEM micrographs of the AgNPs at higher magnification suggested that the synthesized particles had a homogeneous size distribution (**Fig. 1. A and B**). The elemental composition of the particles, shown in the Elemental Dispersive X-Ray Spectroscopy (EDX) images (**Fig. 1.C**),reflects a high silver content present in the NPs study [30].

To identify the functional groups present, Fourier transform infrared spectrometer- (FTIR) was carried out (**Fig. 2. A**) The band at 3340 cm^{-1} was responsible for O-H stretching. The band at 1668 cm^{-1} represent the C = C stretching; furthermore the peak near 1341 cm^{-1} and 810 cm^{-1} represent C-O bending and C-H bending [6].The peaks observed corresponds to the traces of the reductant. The X-ray diffraction studies were followed up to get information about the internal lattice structure of the crystalline metallic silver nanoparticles (**Fig. 2.B**) Herein, the X-ray target was copper (Cu-k^{β}) with an operating voltage and tube current value of 40 kV, 30 mA respectively. The scanning speed was 3 ° / min covering a scan range of 5–90°. The XRD patterns reflected that the synthesized silver nanoparticles have a face centred cubic (FCC) structure that was observed from the diffraction peaks in the 2θ range of 30°–80°, that indexed to (1 1 1),(2 0 0), (2 2 0) [30].To confirm the presence of nanostructured silver particles, the ultraviolet visible spectroscopy was performed using a UV-VIS Spectrophotometer. The absorbance spectra were recorded for a wavelength range of 300–900 nm (**Fig. 2.C**), and it was observed that AgNPs peaks occur at 430nm with high absorbance which is specific for silver nanoparticle [6]. X-ray photoelectron spectroscopy studies (XPS) were executed to analyse the surface composition and to examine the purity of the as synthesized silver nanoparticles extracted from the Tagetes erecta marigold petals (**Fig. 2.D**). The XPS spectrum was recorded in the range of 0–1200 eV. The physico-chemical characterization techniques revealed the formation of silver nanoparticles of 20 nm–50 nm The spectrum shows the presence of metallic silver because of the $3d_{5/2}$ component occurs at the binding energy of 368.3 eV, which represents the characteristic of the metallic oxidation state of Ag [31].

3.2. Electrochemical properties

For investigating the electrochemical performance of the as-prepared material, a series of electrochemical tests were performed. **Fig. 3.A** depicts the Cyclic Voltammetry (CV) curves of PGE and PGE/AgNPs/CS as a working electrode, platinum as a counter electrode and Ag/AgCl as a reference electrode. The CV measurements were carried out in the potential window of 0.5 to - 0.7 V at a scan rate of 50 mV/s. As can be seen, a surface-confined redox peak corresponding to AgNPs is observed at a potential 0.12V and -0.18V vs Ag/AgCl. The redox pair can be attributed to the electron transfer between silver and chitosan matrix, where AgNPs interact with active amino and hydroxyl groups in the CS matrix. The result indicates a large specific capacitance with the prepared material, which might have been obtained from the pseudo-capacitance of the electrochemically activated AgNPs/CS. **Fig. 3.B** shows the corresponding CV curves of PGE/AgNPs/CS at a scan rate in the range of 10–90 mVs^{-1}. Here, the results revealed that the peak current increased linearly as per Randle–Sevick equation [32].

$$i_p = 2.69 \times 10^5 A_e D^{1/2} n^{3/2} V^{1/2} C \quad (2)$$

Where i_p = peak current, n = number of electrons involved in redox reaction, D = diffusion coefficient (7.6×10^{-6} cm^2 s^{-1}), C = concentration of electrolyte, v is the scan rate, A_e is the electrochemically active area of the working electrode, which implies a diffusion-controlled electrochemical process. Upon substitution of various parameters in the above Eq. (2) active area of the working electrode (Ae) was calculated to be 0.24 cm^2 .

The stability and reproducibility of the PGE/AgNPs/CS were also examined. The stability of the PGE/AgNPs/CS was examined after storing the fabricated electrode at a room temperature for 4 weeks, and no significant changes in the current response were observed after the first five days. After 2 weeks of storage time, < 5 % loss was observed. After 4 weeks, 89% of the peak was intact. In order to check the electrode reproducibility, five different electrodes were tested. The relative standard deviation (RSD) of the current response was 1.4 %.

3.3. Supercapacitor application

The hybrid PGE/AgNPs/CS composite showed an enormous scope to be used as a standalone electrode in electrochemical sensing platforms. Meanwhile, to investigate the super capacitive performance of the fabricated PGE/AgNPs/CS electrodes, electrochemical impedance spectroscopy(EIS), galvanostatic charge-discharge(GCD) experiments were carried out using symmetric electrode. The Nyquist plots, shown in the **Fig. 3.C**, suggests that an equivalent series resistance (ESR) (which constitutes the resistance offered by 0.1 M HCl-KCl electrolyte, inherent resistance of the electroactive material, and the contact resistance between the electrode-electrolyte interfaces) for the hybrid PGE/AgNP/Cs composite is significantly smaller than that of bare PGE electrode, which in turn indicates a lower charge transfer resistance. From the EIS plots, the R_{ct} values were estimated to be 50 Ω for the PGE/AgNPs/CS composite as compared to 225 Ω for the bare PGE. The lower charge transfer resistance value of the PGE/AgNPs/CS can be attributed to the formation of a highly conducting membrane with nanostructured silver particles sandwiched between the PGE surface and CS polymer film which enhances the electron transport pathway

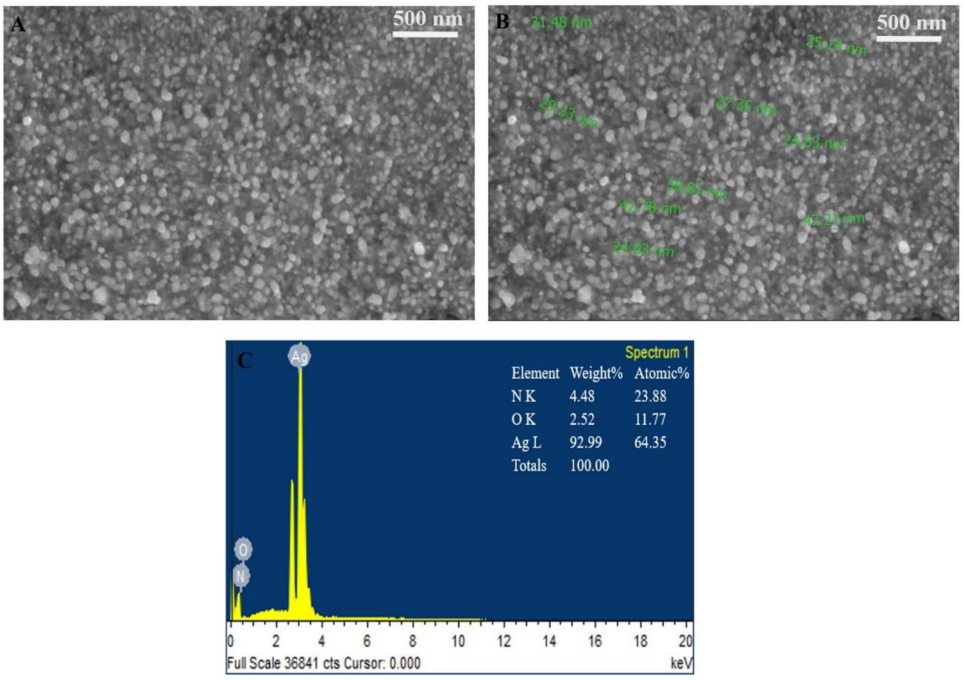

Fig. 1. (A-B) SEM images (C) EDX of AgNPs

between the electrode and the redox probe. To compare the capacitative performance, GCD experiments were carried out for a bare PGE and the hybrid PGE/AgNPs/CS composite at a higher current density of 5 mA cm^{-2}.The results presented in Fig. 3.**D** revealed that the discharge time for the hybrid PGE/AgNPs/CS composite was much higher than a bare PGE yielding a significantly higher areal capacitance value of 150.24 mF cm^{-2} which was an order of magnitude higher when compared to bare PGE (15.36 mF cm^{-2}). Some literature reports suggest, the supercapacitive behaviour of bare PGE at very low current densities, however, when evaluated at higher current densities the bare

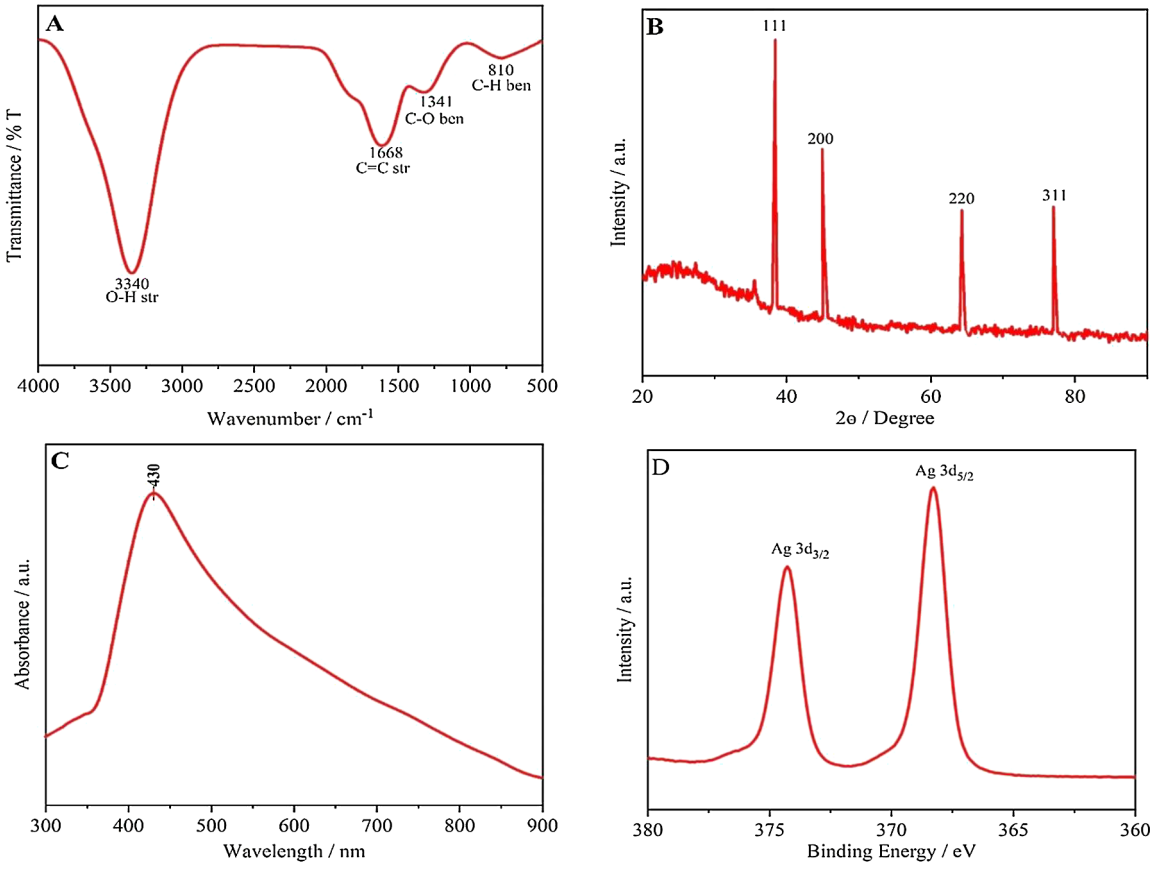

Fig. 2. Synthesized Silver Nanoparticle (A) FTIR Spectra (B) XRD(C) UV-VIS (D) XPS

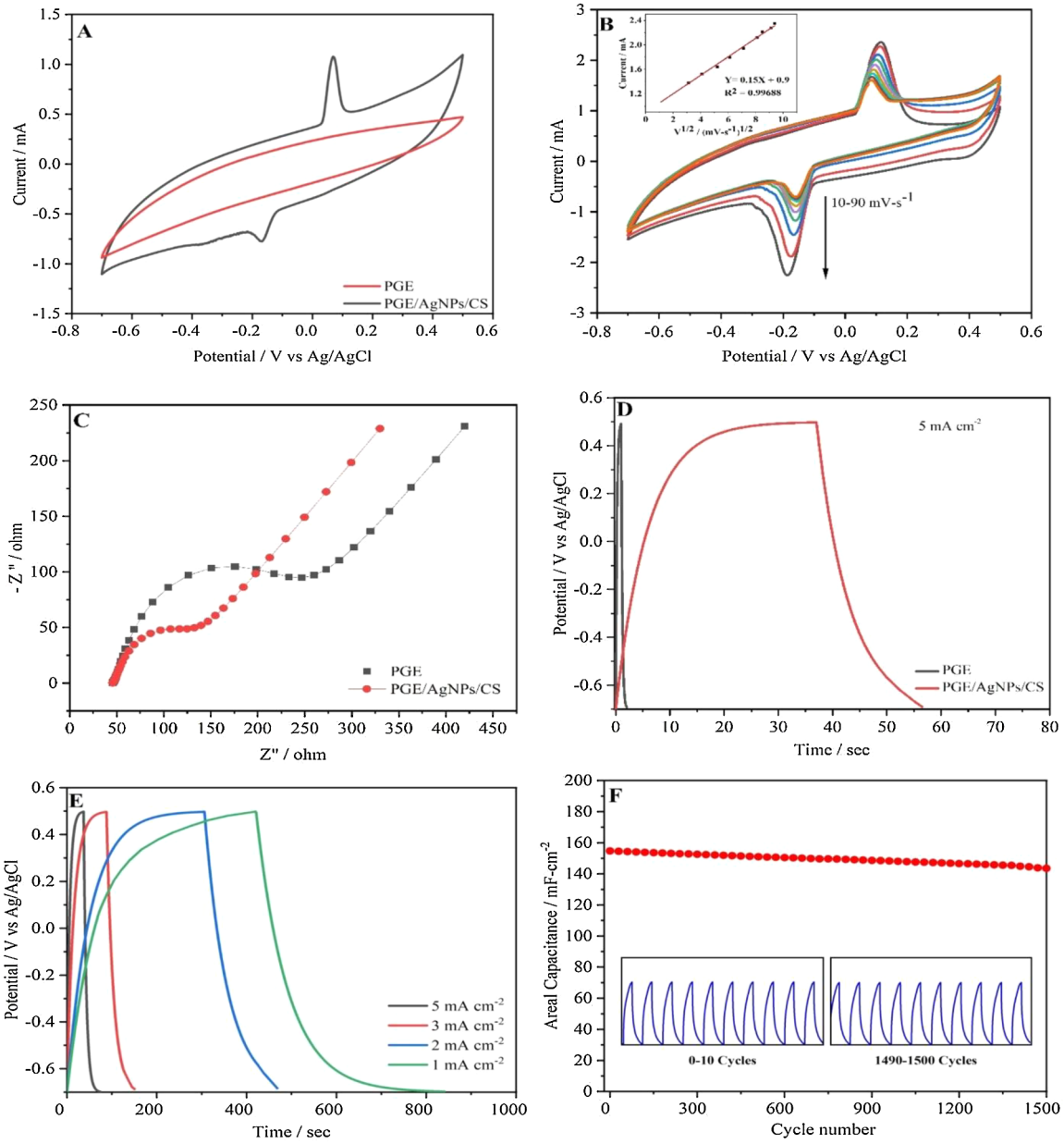

Fig. 3. Effect of potential on CV response in 0.1M HCl/KCl (pH = 2) solution at 10 mV s^{-1} (A) PGE,PGE/AgNPs/CS at 10 mV s^{-1}, (B) Potential cycling experiment within a fixed potential of -0.6 V – 0.4 V with inset plot are respectively of i_{pa} value Vs variable potential, (C) EIS responses of PGE, PGE/AgNPs/CS, (D)GCD curves of a PGE, PGE/AgNPs/CS at 5 mA cm^{-1} (E) GCD curves of a PGE/AgNPs/CS at different current densities, (F) Cycling stability of the PGE/AgNPs/CS electrode. Inset: GCD curves of first and last 10 cycles.

PGE exhibited very low areal capacitance as compared to the hybrid PGE/AgNPs/CS composite [33].

The GCD plots of the hybrid PGE/AgNPs/CS electrodes at different current densities of 1,2,3 and 5 mA cm^{-2} are shown in Fig. 3E. The areal capacitance for the modified PGE electrode was estimated to be 154.67, 200.68. 283.33 and 367.16 mF cm^{-2} at the current densities of 5, 3, 2 and 1 mA cm^{-2}, respectively.The plot depicts that as the current density increases the discharge time of the PGE/AgNPs/CS electrodes decreases. The non-linear shapes of all the curves depict the faradaic battery like capacity shown by the PGE/AgNPs/CS composite. The superior supercapacitative behaviour of hybrid PGE/AgNPs/CS composite and the large operational voltage of 1.2V can be attributed to the rapid surface redox reactions of the silver nanoparticles which has been verified by the CV curves.

Long cycling life is an important criterion in the characterization of supercapacitor electrodes. As shown in Fig. 3.**F** to examine the capacity retention the fabricated PGE/AgNps/CS electrodes, they were cycled upto 1500 cycles. Capacitance system showed minimal deterioration in the charge-discharge rate and capacitance after 1500 cycles with high capacitance retention of 92.8%.The fabrication of the PGE surface with chitosan matrix in the presence of silver nanoparticles provided a better pathway for electron transfer between the bulk electrolyte and the electrode thereby enhancing the storage capacity of the supercapacitor.

To further evaluate the charge and energy storage performance of the PGE/AgNPs/CS a symmetrical supercapacitor device was fabricated by leveragingtwo identical PGE/AgNPs/CS electrodes with pH = 2 HCl-KCl as the liquid electrolyte. Two similar devices were connected in series and were utilized to power a 3V LED for nearly a minute, which shows that the fabricated electrodes have immense potential in portable energy storage applications. The optical micrograph of the glowing LED is shown in **Fig. 4.**

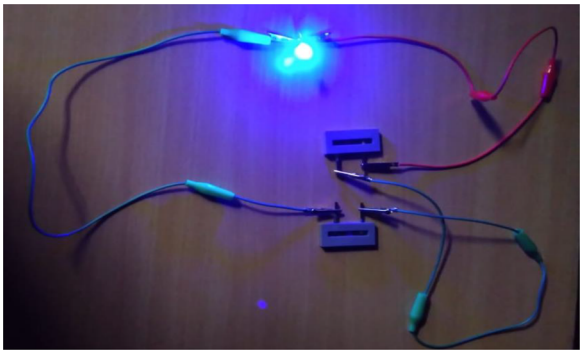

Fig. 4. LED powered by two symmetric electrodes connected in series in a 3D printed microfluidic channel.

3.4. PGE/AgNPs/CS as a H_2O_2 sensor

The prepared hybrid material, PGE/AgNPs/CS, was further explored for H_2O_2 sensing as a model system to investigate the electro catalytic activity of the prepared Ag particles. Prior to the experimental sensing, the test solutions were deaerated with high-purity nitrogen to remove any unwanted peaks due to the presence of diffused oxygen. The three-electrode system consisted of a prepared hybrid material as PGE/AgNPs/CS, Pt and Ag/AgCl as the working, counter and reference electrodes respectively.

As shown in **Fig. 5.A**, in comparison to bare PGE, the modified PGE/AgNPs/CS electrode provided considerable cathodic reduction peak for H_2O_2 reduction. The possible mechanism of H_2O_2 reduction with modified PGE/AgNPs/CS electrode is shown in Scheme 3. Here, AgNPs enhanced the electron transfer activity remarkably leading to H_2O_2 electro-catalysis. Based on previous studies, the mechanism for the electrocatalytic reduction of H_2O_2 in the presence of silver nanoparticles can be described as [34]

$$H_2O_2 \xrightarrow{Ag} \frac{1}{2}O_2 + H_2O$$

$$O_2 + 2_e{}^- + 2H^+ \xrightarrow{Electode} H_2O_2$$

As a result of the above experiments, quantitative analysis of H_2O_2 concentration were performed using cyclic voltammograms (CV) technique in the range of -0.7 to 0.2 V. The solutions were prepared for H_2O_2 in pH 2 HCl-KCl, and a calibration graph was plotted. A linear graph was plotted (**Fig. 5.B**) for concentration over the range of 1 μM -10 μM H_2O_2. As can be seen, the detection limit was found to be 0.51 μM with the prepared hybrid material gives the better catalytic effect of AgNPs in the presence of H_2O_2.

In addition, the effect of variable scan rate on the electro-catalytic reduction of H_2O_2 with PGE/AgNPs/CS was carried out to comprehend the electron transfer mechanism. The peak current increases with the increase in the scan rate within the range of 10-90 mV s^{-1} as shown in **Fig. 5.C** in correspondence with Randle–Sevcikequation [32]. As shown in the inset of **Fig. 5.C**, corresponding calibration plot is linear with slope value -0.602 indicating a diffusion controlled reaction. Further the stability of the electrode was tested after H_2O_2sensing and it was found the peak current sustained post H_2O_2 exposure with <5% reduction (**Fig. 5.D**).

For examining the sensitivity of the modified PGE sensor towards H_2O_2 in a sample containing other interfering species such as ascorbic acid (1mM), uric acid (1mM) dopamine (1mM) and xanthine (1mM), cyclic voltammetry studies were carried out. The results revealed that the interfering species did not produce any observable peaks, therefore, negligible interference from other bio-chemicals is observed. It can be

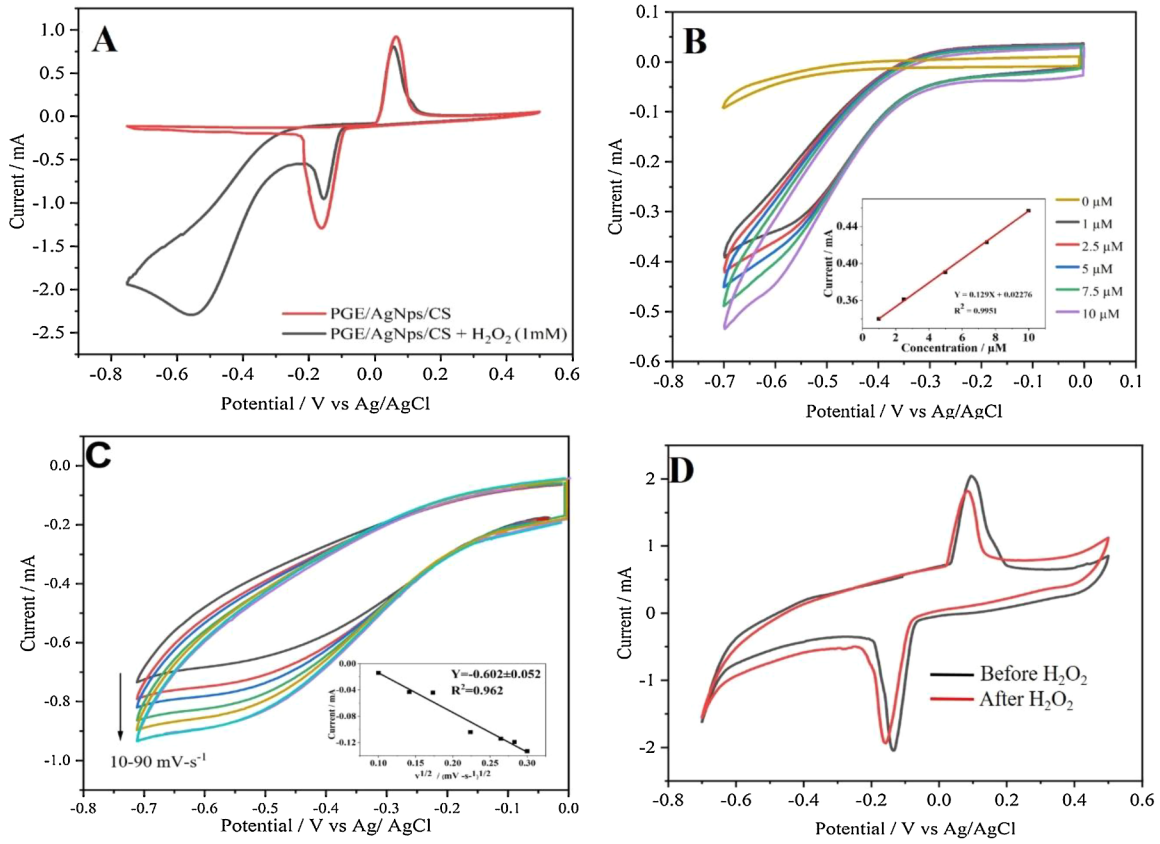

Fig. 5. Effect of potential on CV response in 0.1M HCl/KCl (pH = 2) solution at 10 mV s^{-1} (A) PGE/AgNPs/CS with and without H_2O_2(1 mM) (B) Concentration effect of H_2O_2 on PGE/AgNPs/CS (C) Scan rate effect of PGE/AgNPs/CS in 10 μM H_2O_2 (pH = 2). Inset C, corresponding calibration plot of scan rate vs. $v^{1/2}$. (D) CV response of PGE/AgNPs/CS before and after exposure to 10 μM H_2O_2 (pH = 2) at 50 mV s^{-1}.

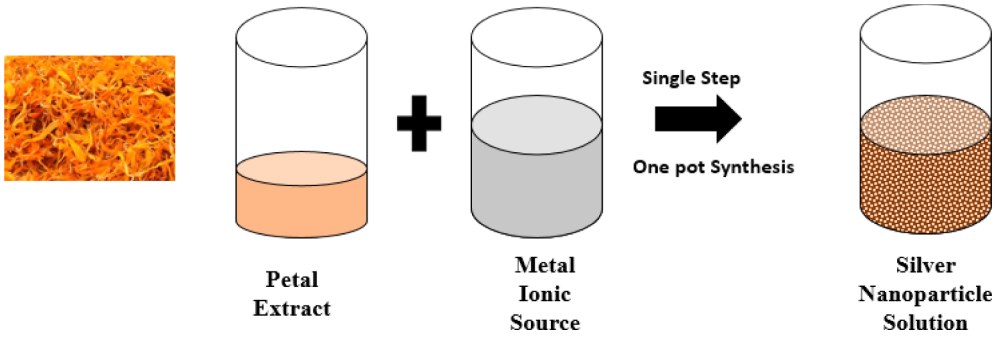

Scheme. 1. Schematic representation of Tagetes based Green Synthesis method for Silver nanoparticle synthesis.

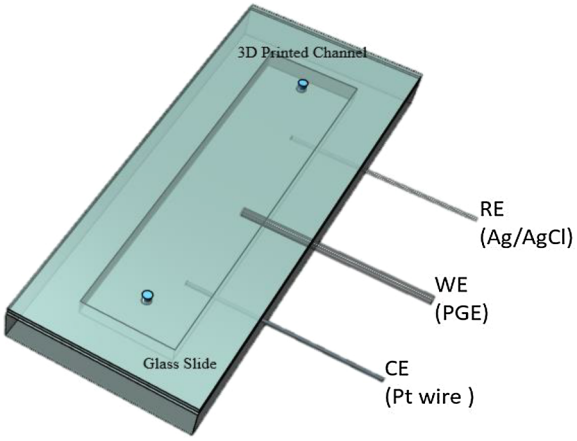

Scheme. 2. Schematic Representation of 3D Microfluidic Channel for Supercapacitor and Electrochemical sensing.

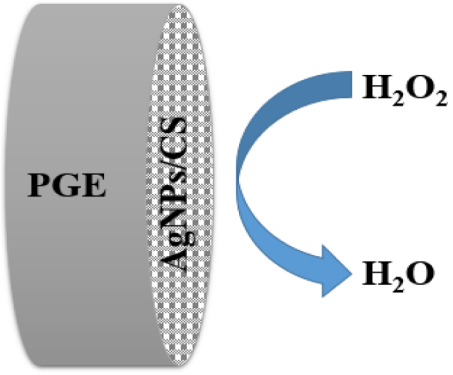

Scheme. 3. Schematic representation of the electrode and overall detection of H_2O_2 by AgNPs.

seen that the PGE/AgNPs/CS sensor is highly selective towards hydrogen peroxide sensing even in the presence of interfering species.

3.5. Real sample analysis

For testing the applicability of the fabricated the PGE/AgNPs/CS electrochemical sensor, three commercially available real samples were tested for H_2O_2 detection in FEM-bleach solution (a), hair dye sample (b) and a medicated H_2O_2 solution (c).

The samples (a) and (b) were prepared by mixing 10 mg of the bleach and 100 mg of the hair dye developer kit in 10 ml of pH 2 HCl-KCl separately, and subsequently sonicated for 15 min, filtered and used. For sample (c) preparation about 10 μM of medicated solution was diluted with 990 μL of pH 2 HCl-KCl. The detected levels and the calculated recovery values in the test samples are presented in the Table 1. From the obtained result, it is suggested that this method can be used for traces analysis of H_2O_2 in cosmetic products in real-time.

Table 1
Real sample analysis.

Samples	Found in original sample(μM)	Spiked (μM)	Detected (μM)	Recovery (%)
Bleach	2.34	5	5.21	104.2
Hair Dye	4.2	5	4.9	98
Medicated H_2O_2	4.56	5	5.02	100.4

4. Conclusion

In summary, the Silver nanoparticles (AgNPs) have been successfully synthesized by using green synthesis technique that delivers large electrochemically active sites and electrical conductivity. A 3DP microfluidic platform was integrated with the electrode. The incorporation of AgNPs on pencil graphite electrodes (PGEs) with chitosan (CS) matrix, was of great benefit for supercapacitor and electrochemical sensing applications. The 3D printed microfluidics platform was used for supercapacitor and electrochemical sensing application with two or three-electrode arrangement. The prepared hybrid material PGE/AgNPs/CS symmetric supercapacitor exhibited electrochemical performance, along with the rapid charge-discharge rate, high specific areal capacitance of 367.16 mF-cm^{-2} at 1 mA-cm^{-2} and exceptional stability of 1500 cyclic lifetime with capacitance retention of92.8%. Also, the PGE/AgNPs/CS provided remarkable electro-catalytic activity towards electrochemical detection of H_2O_2 with LOD of 0.52 μM as compared to other AgNPs based electrodes. The proposed sensor was used to detect H_2O_2 in cosmetic as well as medical samples with high accuracy and selectivity, making it an ideal choice in the development of disposable, low-cost device for hydrogen peroxide detection. The result obtained gave appreciable recovery value suggesting high sensitivity of the electrode towards H_2O_2.

CRediT authorship contribution statement

Mary Salve: Methodology, Data curation, Writing - review & editing. **Aurnab Mandal:** Methodology, Data curation. **Khairunnisa Amreen:** Conceptualization, Writing - review & editing. **Prasant Kumar Pattnaik:** Supervision, Writing - review & editing. **Sanket Goel:** Conceptualization, Investigation, Writing - review & editing.

Declaration of Competing Interest

The authors declare that they have no known competing financial interests or personal relationships that could have appeared to influence the work reported in this paper.

Acknowledgment

The authors thank BITS-Pilani Hyderabad campus for the infrastructure and financial support to carry out the research work. We also acknowledge Central Analytical Laboratory of BITS-Pilani, Hyderabad, for the characterizations. We also acknowledge the Campus Medical Centre for providing the blood serum samples. Khairunnisa Amreen would like to acknowledge DST-SERB NPDF Scheme (PDF/2018/003658) for the financial assistance.

Supplementary materials

Supplementary material associated with this article can be found, in the online version, at doi:10.1016/j.microc.2020.104973.

References

[1] M.H. Rashid, R.R. Bhattacharjee, A. Kotal, T.K. Mandal, Synthesis of spongy gold nanocrystals with pronounced catalytic activities, Langmuir 22 (2006) 7141–7143, https://doi.org/10.1021/la060939j.
[2] A.K. Khan, R. Rashid, G. Murtaza, A. Zahra, Gold nanoparticles: synthesis and applications in drug delivery, Trop. J. Pharm. Res. 13 (2014) 1169–1177, https://doi.org/10.4314/tjpr.v13i7.23.
[3] P.M. Anjana, M.R. Bindhu, R.B. Rakhi, Green synthesized gold nanoparticle dispersed porous carbon composites for electrochemical energy storage, Mater. Sci. Energy Technol. 2 (2019) 389–395, https://doi.org/10.1016/j.mset.2019.03.006.
[4] H. Yazid, R. Adnan, S.A. Hamid, M.A. Farrukh, Synthesis and characterization of gold nanoparticles supported on zinc oxide via the deposition-precipitation method, Turk. J. Chem. 34 (2010) 639–650, https://doi.org/10.3906/kim-0912-379.
[5] K. Jyoti, M. Baunthiyal, A. Singh, Characterization of silver nanoparticles synthesized using Urtica dioica Linn. Leaves and their synergistic effects with antibiotics, J. Radiat. Res. Appl. Sci. 9 (2016) 217–227, https://doi.org/10.1016/j.jrras.2015.10.002.
[6] P. Prakash, P. Gnanaprakasam, R. Emmanuel, S. Arokiyaraj, M. Saravanan, Green synthesis of silver nanoparticles from leaf extract of Mimusops elengi, Linn. For enhanced antibacterial activity against multi drug resistant clinical isolates, Colloids Surf. B 108 (2013) 255–259, https://doi.org/10.1016/j.colsurfb.2013.03.017.
[7] D.S. Patil, S.A. Pawar, R.S. Devan, S.S. Mali, M.G. Gang, Y.R. Ma, C.K. Hong, J.H. Kim, P.S. Patil, Polyaniline based electrodes for electrochemical supercapacitor: Synergistic effect of silver, activated carbon and polyaniline, J. Electroanal. Chem. 724 (2014) 21–28, https://doi.org/10.1016/j.jelechem.2014.04.006.
[8] L. Tang, F. Duan, M. Chen, Green synthesis of silver nanoparticles embedded in polyaniline nanofibers via vitamin C for supercapacitor applications, J. Mater. Sci. Mater. Electron. 28 (2017) 7769–7777, https://doi.org/10.1007/s10854-017-6472-y.
[9] K. Mallikarjuna, G. Narasimha, G.R. Dillip, B. Praveen, B. Shreedhar, C. Sree Lakshmi, B.V.S. Reddy, B. Deva Prasad Raju, Green synthesis of silver nanoparticles using Ocimum leaf extract and their characterization, Dig. J. Nanomater. Biostruct. 6 (2011) 181–186.
[10] H. Padalia, P. Moteriya, S. Chanda, Green synthesis of silver nanoparticles from marigold flower and its synergistic antimicrobial potential, Arab. J. Chem. 8 (2015) 732–741, https://doi.org/10.1016/j.arabjc.2014.11.015.
[11] S. Dhibar, C.K. Das, Silver nanoparticles decorated polypyrrole/graphene nanocomposite: a potential candidate for next-generation supercapacitor electrode material, J. Appl. Polym. Sci. 134 (2017) 1–14, https://doi.org/10.1002/app.44724.
[12] Y.C. Chen, J.H. Hsu, Y.G. Lin, Y.K. Hsu, Synthesis of Fe_2O_3 nanorods/silver nanowires on coffee filter as low-cost and efficient electrodes for supercapacitors, J. Electroanal. Chem. 801 (2017) 65–71, https://doi.org/10.1016/j.jelechem.2017.07.032.
[13] G. Wang, L. Zhang, J. Zhang, A review of electrode materials for electrochemical supercapacitors, Chem. Soc. Rev. 41 (2012) 797–828, https://doi.org/10.1039/c1cs15060j.
[14] S.T.P. Devarenne, A. Han, S. Darwin, R. Reyes, D.R. Reyes, A. Folch, H. Minhas, M. Gaitan, J. Stubbs, A. Lee, H. Andersson-svahn, M. Gilligan, E. Wilson, Lab on a chip lab on a chip, Lab Chip 24 (2014) 1381–1388, https://doi.org/10.1039/C4LC01038H.
[15] Y. Liu, X. Peng, Recent advances of supercapacitors based on two-dimensional materials, Appl. Mater. Today 7 (2017) 1–12, https://doi.org/10.1016/j.apmt.2017.01.004.
[16] L.L. Zhang, X.S. Zhao, Carbon-based materials as supercapacitor electrodes, Chem. Soc. Rev. 38 (2009) 2520–2531, https://doi.org/10.1039/b813846j.
[17] J.R. Miller, P. Simon, Materials science: Electrochemical capacitors for energy management, Science 321 (2008) 651–652, https://doi.org/10.1126/science.1158736.
[18] K. Wang, M. Xu, M. Shrestha, Z. Gu, Q.H. Fan, Plasma-assisted fabrication of graphene in ambient temperature for symmetric supercapacitors application, Mater. Today Energy 4 (2017) 7–13, https://doi.org/10.1016/j.mtener.2017.03.001.
[19] K.A. Owusu, L. Qu, J. Li, Z. Wang, K. Zhao, C. Yang, K.M. Hercule, C. Lin, C. Shi, Q. Wei, L. Zhou, L. Mai, Low-crystalline iron oxide hydroxide nanoparticle anode for high-performance supercapacitors, Nat. Commun. 8 (2017) 1–11, https://doi.org/10.1038/ncomms14264.
[20] X. Zhang, Z. Lin, B. Chen, W. Zhang, S. Sharma, W. Gu, Y. Deng, Solid-state flexible polyaniline/silver cellulose nanofibrils aerogel supercapacitors, J. Power Sources 246 (2014) 283–289, https://doi.org/10.1016/j.jpowsour.2013.07.080.
[21] V.C. Hoang, V.G. Gomes, High performance hybrid supercapacitor based on doped zucchini-derived carbon dots and graphene, Mater. Today Energy 12 (2019) 198–207, https://doi.org/10.1016/j.mtener.2019.01.013.
[22] M. Javed, S.M. Abbas, S. Hussain, M. Siddiq, D. Han, L. Niu, Amino-functionalized silica anchored to multiwall carbon nanotubes as hybrid electrode material for supercapacitors, Mater. Sci. Energy Technol. 1 (2018) 70–76, https://doi.org/10.1016/j.mset.2018.03.002.
[23] E. Hür, G.A. Varol, A. Arslan, The study of polythiophene, poly(3-methylthiophene) and poly(3,4-ethylenedioxythiophene) on pencil graphite electrode as an electrode active material for supercapacitor applications, Synth. Met. 184 (2013) 16–22, https://doi.org/10.1016/j.synthmet.2013.09.028.
[24] P. Tang, L. Han, L. Zhang, Facile synthesis of graphite/PEDOT/MnO2 composites on commercial supercapacitor separator membranes as flexible and high-performance supercapacitor electrodes, ACS Appl. Mater. Interfaces 6 (2014) 10506–10515, https://doi.org/10.1021/am5021028.
[25] P. Liu, J. Liu, S. Cheng, W. Cai, F. Yu, Y. Zhang, P. Wu, M. Liu, A high-performance electrode for supercapacitors: silver nanoparticles grown on a porous perovskite-type material La 0.7 Sr 0.3 $CoO_3-\Delta$ substrate, Chem. Eng. J. 328 (2017) 1–10, https://doi.org/10.1016/j.cej.2017.06.150.
[26] J.K. Gan, Y.S. Lim, N.M. Huang, H.N. Lim, Boosting the supercapacitive properties of polypyrrole with chitosan and hybrid silver nanoparticles/nanoclusters, RSC Adv. 6 (2016) 88925–88933, https://doi.org/10.1039/c6ra13697d.
[27] F. Sun, X. Pang, I. Zhitomirsky, Electrophoretic deposition of composite hydroxyapatite-chitosan-heparin coatings, J. Mater. Process. Technol. 209 (2009) 1597–1606, https://doi.org/10.1016/j.jmatprotec.2008.04.007.
[28] F. Meng, H. Yin, Y. Li, S. Zheng, F. Gan, G. Ye, One-step synthesis of enzyme-stabilized gold nanoclusters for fluorescent ratiometric detection of hydrogen peroxide, glucose and uric acid, Microchem. J. 141 (2018) 431–437, https://doi.org/10.1016/j.microc.2018.06.006.
[29] A. Sukeri, A.S. Lima, M. Bertotti, Development of non-enzymatic and highly selective hydrogen peroxide sensor based on nanoporous gold prepared by a simple unusual electrochemical approach, Microchem. J. 133 (2017) 149–154, https://doi.org/10.1016/j.microc.2017.03.023.
[30] Z.H. Pak, H. Abbaspour, N. Karimi, A. Fattahi, Eco-friendly synthesis and antimicrobial activity of silver nanoparticles using Dracocephalum moldavica seed extract, Appl. Sci. (Switz.) 6 (2016), https://doi.org/10.3390/app6030069.
[31] D.G. Larrude, M.E.H. Maia Da Costa, F.L. Freire, Synthesis and characterization of silver nanoparticle-multiwalled carbon nanotube composites, J. Nanomater. 2014 (2014), https://doi.org/10.1155/2014/654068.
[32] M.Z.M. Nasir, M. Pumera, Impact electrochemistry on screen-printed electrodes for the detection of monodispersed silver nanoparticles of sizes 10–107 nm, PCCP 18 (2016) 28183–28188, https://doi.org/10.1039/c6cp05463c.
[33] N. Vishnu, A. Gopalakrishnan, S. Badhulika, Impact of intrinsic iron on electrochemical oxidation of pencil graphite and its application as supercapacitors, Electrochim. Acta 269 (2018) 274–281, https://doi.org/10.1016/j.electacta.2018.03.024.
[34] B. Zhan, C. Liu, H. Shi, C. Li, L. Wang, W. Huang, X. Dong, A hydrogen peroxide electrochemical sensor based on silver nanoparticles decorated three-dimensional graphene, Appl. Phys. Lett. 104 (2014) 2–7, https://doi.org/10.1063/1.4884418.